Catalysis Science & Technology

Accepted Manuscript

ROYAL SOCIETY OF CHEMISTRY

www.rsc.org/catalysis

Realization of high effective Pd-Cu-Cl_x/Al_2O_3 catalyst for low temperature CO oxidation by pre-synthesizing the active copper phase of $Cu_2Cl(OH)_3$

Xuexun Du,[a] Huiying Li,[a] Jun Yu,[a] Xiuzhen Xiao,[a] Zhangping Shi,[a] Dongsen Mao,[a] Guanzhong Lu*[ab]

[a] Research Institute of Applied Catalysis, School of Chemical and Environmental Engineering, Shanghai Institute of Technology, Shanghai 201418, China.

[b] Key Laboratory for Advanced Materials and Research Institute of Industrial catalysis, East China University of Science and Technology, Shanghai 200237, China.

*Corresponding Author: Fax: +86-21-64252923. E-mail: gzhlu@ecust.edu.cn (G.Z. Lu).

Abstract: The Pd-Cu-Cl_x/Al_2O_3 catalysts (PCC) were prepared by the two-step impregnation (TI) in the organic solvent, wet impregnation (WI) and NH_3 coordination-impregnation (CI) method, respectively. The PCC-TI catalyst prepared by the two-step impregnation method (TI) exhibited much higher activity and stability for CO oxidation than other catalysts, resulting from the smaller size of $Cu_2Cl(OH)_3$ and less carbonates deposited on the surface of PCC-TI catalyst. Using PCC-TI catalyst, the complete conversion temperature of CO was 10 °C in the presence of 3.1%H_2O. Among the three catalysts, the activation energy (E_a) of PCC-TI/ethanol was the lowest (27.1 kJ/mol). The PCC-TI/ethanol prepared in the ethanol solvent showed a higher activity compared with PCC-TI/methanol, due to much stronger interaction between the copper and palladium species. High concentrations of moisture and CO played negative effects on the CO conversion. The former was coming from excessive −OH groups (from H_2O dissociation) occupied the active sites of Pd and Cu, though −OH groups can work as parts of the catalytic cycle, and the latter might be originated from the competitive adsorption and carbonates covered on the surface. We took DFT calculation to study the adsorption of H_2O and CO on the surface, and the catalytic cycle of CO oxidation on the Pd species, revealing the possibly evolutive routes for the common species observed in *in situ* DRIFTS spectra.

Keywords: Pd-Cu-Cl_x/Al_2O_3 catalyst; CO oxidation; Two-step impregnation method; Active phase of $Cu_2Cl(OH)_3$; Catalyst preparation.

1. Introduction

Low temperature catalytic oxidation of CO has aroused more and more attentions, because of its wide applications and scientific researches, such as automotive exhaust purification, room air cleaning and carbon monoxide leak detection.[1-3] Among various catalysts for CO oxidation, the hopcalite catalyst (Cu-Mn mixed oxide) and Co_3O_4 exhibit the excellent catalytic activity at room temperature and/or low temperature.[4-6] However, the most frustrating thing is that these catalysts would deactivate rapidly in the reactant gas containing a trace amount of moisture.[6-8] In the real environment, the moisture content is often closed to saturated-steam, water non-resistance for the catalysts seriously limits their practical application. Nano-gold catalysts have been studied warmly since it was pioneeringly reported by Haruta,[9] and showed outstanding activity and stability for low temperature CO oxidation even in the humid condition. However, gold nanoparticle catalysts also have some disadvantages, such as sintering of the gold particles, rapid deactivation under halogen-including atmosphere, the decline of the activity with time on stream, and high cost as a precious metal.[9-12] Hence, research and development of CO oxidation catalyst with high activity and stability is very significant for further practical applications.

The heterogeneous Wacker-type catalyst (supported Pd-Cu-Cl_x) is another attractive catalyst for low temperature CO oxidation, because of its excellent stability in the presence of moisture and halogen compounds, which has been widely researched and reported.[13-22] It was currently identified that $Cu_2Cl(OH)_3$ species played vital roles in the supported Pd-Cu-Cl_x catalyst. Lee *et al.* found that the $Cu_2Cl(OH)_3$ phase on the carbon support was a more effective copper species compared with the $CuCl_2.2H_2O$ phase, and could reoxidize the reduced palladium species (Pd^0) via Wacker cycle.[16] We have found that in the Pd-Cu-Cl_x/Al_2O_3 catalyst prepared by a NH_3 coordination-impregnation method, the presence of active $Cu_2Cl(OH)_3$ species could enhance the determining step rate from Pd^0 to Pd^+ in the Wacker-type cycle for CO oxidation.[19] In order to achieve the $Cu_2Cl(OH)_3$ active phase, researchers have conducted lots of work. For instance, Kim *et al.* investigated the effect of support (as silica, alumina and carbon) on the catalytic property, and

found silica was a less active support compared with alumina and carbon, because the active copper species of $Cu_2Cl(OH)_3$ could not be stabilized on silica support.[14] Park and Lee used carbon pretreated with HNO_3 as the support of this catalyst due to the enrichment of the carboxylic and carbonyl groups on its surface, and/or $Cu(NO_3)_2$ as a copper precursor to prepare this catalyst, which helped to the formation of $Cu_2Cl(OH)_3$ phase.[17] Up to now, many researches mainly focused on the influences of the support and precursor on a formation of active $Cu_2Cl(OH)_3$ phase, but directly using the $Cu_2Cl(OH)_3$ phase pre-synthesized to prepare Pd-Cu-Cl_x/Al_2O_3 catalyst has not been reported yet. In this paper, the active copper phase of $Cu_2Cl(OH)_3$ was synthesized alone, and then supported on the Al_2O_3 surface to prepare the bimetallic catalyst with an excellent activity and stability for the room temperature CO oxidation even in the presence of high concentration of moisture.

Herein, the Pd-Cu-Cl_x/Al_2O_3 catalysts were prepared by a two-step impregnation method with different solvents, and their physicochemical and catalytic properties for low temperature CO oxidation were studied to understand the effect of the active copper phase on the catalytic performance. Based on the experiment results, the influences of physicochemical properties of catalysts on their catalytic performances, kinetics characters, the surface reaction *etc*. were discussed in detail. While we took DFT calculation[23] to study the adsorption of H_2O and CO on the surface, and the catalytic cycle of CO oxidation on the Pd species, to reveal the possibly evolutive routes for the common species observed in the DRIFTS spectra.

2. Experimental section

2.1. Catalyst preparation

$CuCl_2$ (AR), methanol (AR), ethanol (AR) and propylene oxide (AR) were purchased from Sinoharm Chemical Reagent Co., Ltd.; $PdCl_2$ (AR) from Adamas Reagent Co., Ltd., and Al_2O_3 (WHA-204, BET surface area of 194 m^2/g) from Wenzhou Jingjing aluminum Ltd.

1.7wt%Pd-3.3wt%Cu-Cl_x/Al_2O_3 catalyst was prepared by the two-step impregnation (TI) method.

Firstly, $Cu_2Cl(OH)_3$ was synthesized with the reported method:[24] weighed $CuCl_2$ was dissolved in 2 mL mixed solution of propylene oxide and alcohol (methanol or ethanol) (volume ratio of propylene oxide/alcohol was 1/1), a pale green turbid liquid was formed after 10 min of adding $CuCl_2$. Then 1g Al_2O_3 was impregnated in this solution. After being aged for 24 h, the $Cu_2Cl(OH)_3/Al_2O_3$ sample was dried at room temperature and calcined at 300 °C for 4 h.

Weighed $PdCl_2$ was dissolved in 2 mL 0.1 M hydrochloric acid, and then $Cu_2Cl(OH)_3/Al_2O_3$ sample was impregnated in this $PdCl_2$ solution and dried at 25 °C for 12 h. This 1.7wt.%Pd-3.3wt.%Cu-Cl_x/Al_2O_3 catalyst sample was denoted as PCC-TI/methanol or PCC-TI/ethanol.

This Pd-Cu-Cl_x/Al_2O_3 catalyst was also prepared by the conventional wet impregnation method in the water solvent, and NH_3 coordination-impregnation method in the isopropanol solvent, which were denoted as PCC-WI and PCC-CI, respectively.

2.2. Catalyst characterization

The actual contents of Cu and Pd in catalysts were measured with inductively coupled plasma optic emission spectrometry (ICP-OES) on a PerkinElmer Optima 7000 DV. The surface areas of samples were measured by N_2 adsorption at -196 °C on a Micrometrics ASAP 2020 M+C adsorption apparatus and calculated by the Brumauer–Emmett–Teller (BET) method. The X-ray powder diffraction (XRD) patterns of catalysts were performed on a PANalytical X'Pert Pro MRD X-ray diffractometer with CuKα radiation (λ=0.154056 nm) operated at 40 kV and 40 mA. The mean crystalline sizes of Cu species in the catalysts were estimated by Scherrer equation on the basis of the broadening of diffraction peaks.

Hydrogen temperature-programmed reduction (H_2-TPR) of sample was tested in the continuous-flow apparatus equipped with TCD detector. 100 mg of catalyst was packed in the quartz micro-reactor and pretreated in a N_2 flow of 30 mL/min at 30 °C for 0.5 h. Then the sample was heated up to 500 °C at 10 °C/min in the mixture gas of 10% H_2/N_2 (30 mL/min).

In situ diffuse reflectance infrared Fourier transforms spectroscopy (DRIFTS) spectra were

gained at room temperature on a Nicolet 6700 FT-IR spectrometer equipped with a MCT detector, in which the spectral resolution was 4 cm^{-1} and scan number was 64 time. The DRIFTS cell (Harrick) was fitted with CaF_2 windows and a heating cartridge that allowed samples to be heated to 400 °C. The sample was pretreated in N_2 (50 mL/min) at 25 °C for 1 h, then the background spectrum was collected in the N_2 atmosphere. After the reactant gas of 0.15% CO-20%O_2-3.1%H_2O/balanced N_2 (50 mL/min) flowed through the sample cell, the IR absorption spectra on the catalysts were recorded at 25 °C.

2.3. Computational details of DFT study

The DFT calculations were done by the help of the VASP. The generalized gradient approximation (GGA) was used to solve the Kohn-Sham equations. The project-augmented wave (PAW) method was adopted to represent the core-valence interaction.[25] Like the model used by Digne *et al*.,[26] herein, the optimized lattice parameters of γ-Al_2O_3 were taken as a = 5.57, b = 8.39, c = 8.05, β = 90.598, and the (100) facet was selected as the calculation model, in which a 6-layer slab model contained 24 Al_2O_3 units and the vacuum region between the slabs was set to 16 Å. The valence electronic states were expanded in plane wave basis sets with an energy cut-off at 450 eV. The force threshold for the optimization and transition state search was 0.05 eV/Å. Only the top two atomic layers of the slab and their adsorbates are allowed to relax, that is to say, the bottom 4 layers are fixed. A $p(1\times2)$ surface cell of 1×1×1 k-point mesh with an area of 11.17 × 8.41 $Å^2$ was used to fully take the relaxation effects into account. Two criteria were used for searching the transition states by using a constrained optimization scheme: (a) all forces on atoms vanished, and (b) the total energy was a maximum along the reaction coordination but a minimum with regard to the rest of freedom degrees.

2.4. Testing of the catalyst performance and kinetic characters

The performances of catalysts for CO oxidation were tested in a quartz tubular fixed-bed reactor (Ø5 mm). The sample (200 mg, 20-40 mesh) was packed in the reactor with quartz wool at both sides of the catalyst. The mixture gas of 1500 ppm CO/air was used as the reactant gas, and its

flow rate was 50 mL/min, corresponding to the WHSV of 15,000 mL/(g·h). Before entering the reactor, the feed gas flowed through a water vapor saturator. The water concentration in the reactant gas could be adjusted from 0.6% to 3.1% by changing the temperature of water vapor saturator. The CO concentration was monitored by online gas chromatograph (GC) equipped with a FID detector, in which the methanizer was used for hydrogenating CO_2 and CO to methane. The CO conversion was tested after 10 min of reaction. The CO conversion, X (%) = (CO_{inlet} - CO_{outlet})/CO_{inlet} × 100%, CO_{inlet} was the initial CO concentration in the inlet, and CO_{outlet} means the CO concentration in the outlet.

The kinetic data was measured in the same reactor as the catalytic performance testing. Based on the differential reactor mode, the CO conversion was controlled at less than 15%. The reactant gas consisted of 1500 ppm CO + 3.1% H_2O/air. After the steady operation for 30 min, the reaction rates were tested. The oxidation rate of CO, r (mol/(g·h)) = (N_{CO} × X)/W_{cat}, where N_{CO} is the CO flow rate (mol/h), W_{cat} is the catalyst weight (g), X is the CO conversion (%). When the CO conversion was < 15%, the influence of produced CO_2 and H_2O on the reaction rate (r) might be ignored; hence, the empirical equation of reaction rate for CO oxidation could be measured as equation 1.

$$r = \mathrm{A}\exp\left(-\frac{E_a}{RT}\right)P_{CO}^{\alpha}P_{O_2}^{\beta} \quad (1)$$

Taking the logarithm of equation 1, equation 2 can be obtained.

$$\ln r = \ln \mathrm{A} + \alpha \ln P_{CO} + \beta \ln P_{O_2} - E_a/\mathrm{RT} \quad (2)$$

In the process of kinetics data testing, the composition of reactant gas remained unchanged basically, and the CO conversion was < 15%, therefore, lnA, $\alpha \ln P_{CO}$ and $\beta \ln P_{O2}$ could be regarded as approximately constants, and equation 2 can be simplified to $\ln r = -E_a/\mathrm{RT} + \mathrm{C}$. The activation energy (E_a) can be obtained from the slope of the resulting linear plot of ln r versus 1/T.

3. Results and discussions

3.1. Influence of preparation method on the catalytic activity and stability

Fig.1 shows the influence of preparation methods on the catalytic performances of Pd-Cu-Cl_x/Al_2O_3 catalysts for CO oxidation (1500 ppm CO and ~3.1% water/air). As shown in Fig.1A, the CO conversion over the PCC-WI catalyst prepared by wet impregnation method reached a maximum (~83%) at 20 °C, and then decreased with an increase in the reaction temperature, because of the losses of water and chlorine at a relatively high temperature during the reaction.[27] For other three Pd-Cu-Cl_x/Al_2O_3 catalysts prepared by NH_3 coordination-impregnation and two-step impregnation method, the PCC-TI/ethanol exhibited higher catalytic activity: CO was completely converted at 20 °C (T_{100}) over the PCC-CI or PCC-TI/methanol, and T_{100} over PCC-TI/ethanol was only ~10 °C.

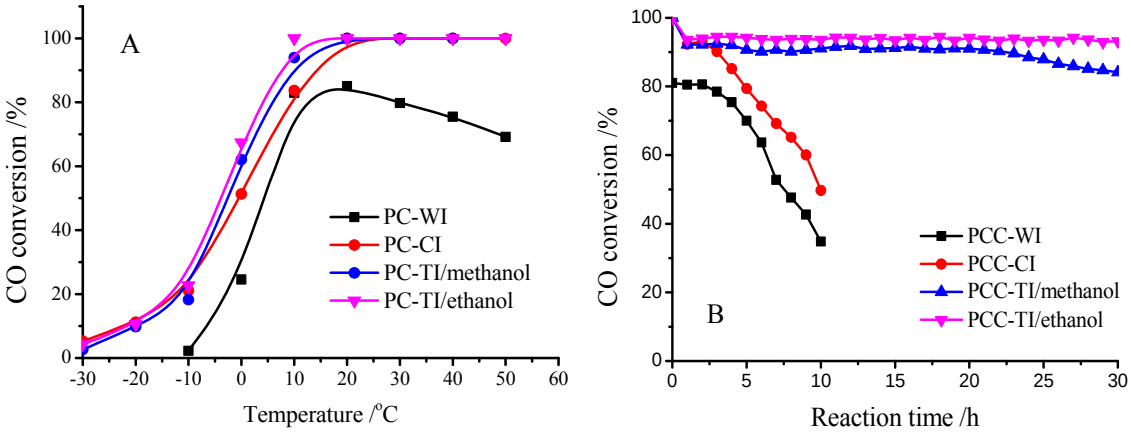

Fig. 1. Influence of the preparation method on the catalytic performances of Pd-Cu-Cl_x/Al_2O_3 catalysts for the CO oxidation in the reactant gas of 1500 ppm CO and ~3.1% moisture/air at 25 °C.

The catalytic stability for CO oxidation was also investigated at 25 °C and the reactant gas was 1500 ppm CO and ~3.1% water/air, and the results are shown in Fig. 1B. For the PCC-WI catalyst, the CO conversion was only ~83% after 2 h of reaction, and decreased to ~30% after 10 h. For the PCC-CI catalyst, the CO conversion can be maintained at ~93% for 2 h, and then decreased to ~43% after 10 h. When the two-step impregnation method was employed to prepare the Pd-Cu-Cl_x/Al_2O_3 catalyst, its catalytic stability was improved significantly. For the PCC-TI/methanol catalyst, the CO conversion could be maintained above 90% for 22 h of reaction. Using the PCC-TI/ethanol catalyst, the CO conversion was hardly changed after 30 h of reaction and kept at above 93%.

3.2. Influence of moisture on the CO catalytic oxidation

The PCC-TI/ethanol catalyst was used as a model catalyst to investigate the influence of moisture on the CO catalytic oxidation at 25 °C. As shown in Fig. 2, in the presence of ~0.6% moisture, the catalytic activity of PCC-TI/ethanol could keep at above 93% for 100 h. In the presence of ~3.1% moisture, its catalytic activity was unchanged for 30 h, and then gradually decreased from ~93% to ~58% CO conversion within 30 h.

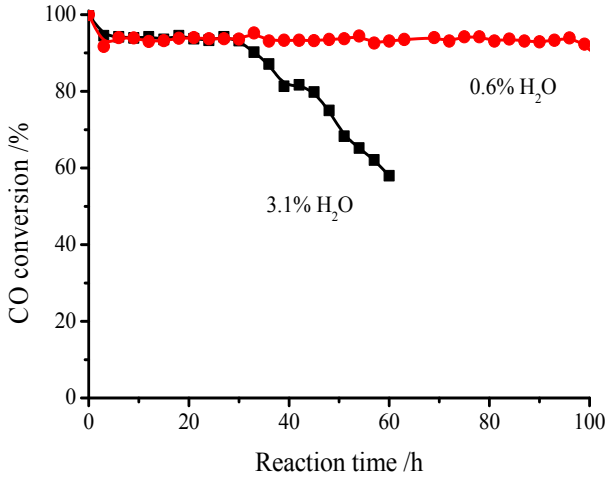

Fig. 2. The CO conversion over the PCC-TI/ethanol catalyst in the reactant gas of 1500 ppm CO and 0.6 or 3.1% moisture/air at 25 °C.

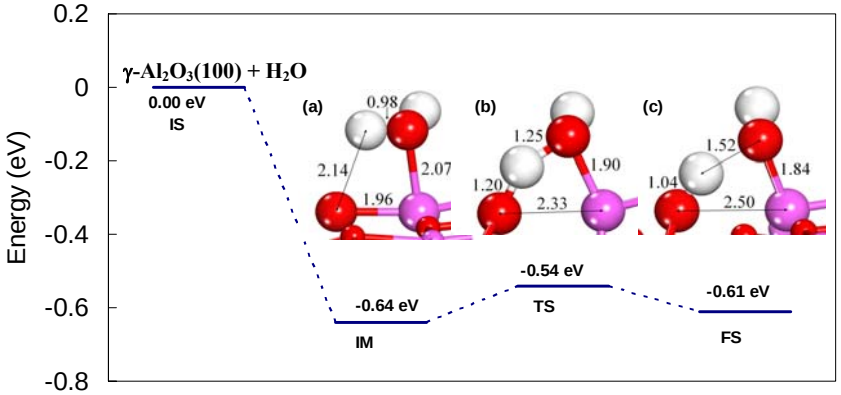

Fig. 3. The energy change and corresponding structures for the H_2O dissociation ($-H_2O \rightarrow -H + -OH$) on the $Al_2O_3(100)$ facet. (a) Structure of adsorbed H_2O; (b) transition state for H_2O dissociation; (c) structure of dissociated H_2O. (Unit of bond length is Å. O atoms are red, Al atoms are pink, H atoms are white).

These results clearly show that, in the presence of relatively high concentration of moisture, the catalytic oxidation of CO would be inhibited, that is to say, the catalyst would be deactivated. To further understand this phenomenon, theoretical calculation with DFT for water adsorption and

dissociation on the dry γ-Al_2O_3 (100) facet was performed. Structures and energy diagram of adsorbed H_2O (IM), transition state for H_2O dissociation (TS) and H_2O dissociated (FS) are shown in Figure 3. We can see, that IM was dissociated through a TS with small energy barrier (0.10 eV), indicating that a formation of hydroxylated (100) facet of γ-Al_2O_3 is kinetically favored. In this way, the presence of excess H_2O would easily dissociate to −H and −OH, which can occupy the active sites of Pd and Cu on the Al_2O_3 surface as poisonous species, resulting in a deactivation of the Pd-Cu-Cl_x/Al_2O_3 catalyst for the CO oxidation.[7,21] However, the negative effect of the excess of H_2O does not mean that water is dispensable in this process of low-temperature CO oxidation. On the contrary, the proton –H on the O_{3c} site and –OH group on the Al_{5c} site which are dissociated from a certain amount of H_2O, can work as parts of the catalytic cycle as an important species for low temperature CO oxidation over the Pd-Cu-Cl_x/Al_2O_3 catalyst.[23,28]

3.3. Influence of CO concentration on the CO catalytic oxidation

Fig. 4 shows the influence of CO concentration on the CO oxidation over the PCC-TI/ethanol catalyst at 25 °C. The results show that, ~89% CO conversion can be maintained after 30 h of reaction when 750 ppm CO was used; when the CO concentration was increased from 750 ppm to 1500 ppm, the CO conversion was increased from ~89% to ~94% and maintained after 30 h of reaction; when the CO concentration reached 3000 ppm, ~95% CO conversion could only be maintained for 5 h, and then CO conversion was gradually decreased from ~95% to ~80% in the following 25 h.

The above results clearly demonstrated the negative influence of relatively high CO concentration on the CO oxidation over the PCC-TI/ethanol catalyst. When the CO concentration was increased from 750 ppm to 1500 ppm, the CO conversion increased gradually, and when the CO concentration continually increased to 3000 ppm, more CO would react with oxygen to form surface carbonates which remained on the surface without timely decomposition to gaseous CO_2. Over the Pd-Cu-Cl_x/Al_2O_3 catalyst, CO_2 could only form carbonates on the acidic Al_2O_3 surface, and cover the active sites or block the pores.[22] Hence, the covering of carbonates and the

competitive adsorption between CO and CO_2 on the catalyst surface might be main reasons for the negative influence of the relatively high CO concentration on the catalytic oxidation of CO.

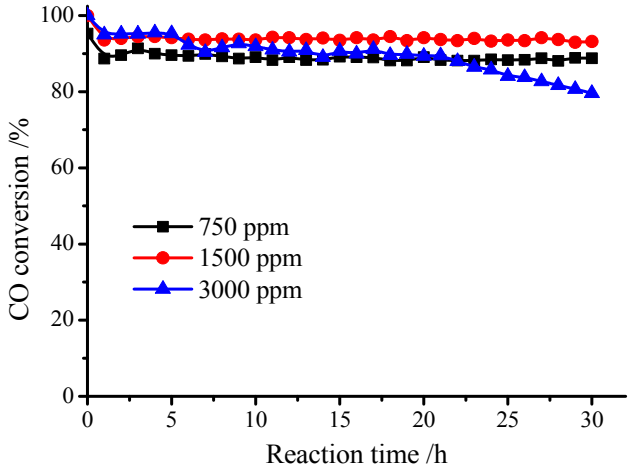

Fig. 4. Influence of the CO concentration on the CO oxidation over the PCC-TI/ethanol catalyst at 25 °C with ~3.1% moisture/air.

3.4. Reaction kinetic character

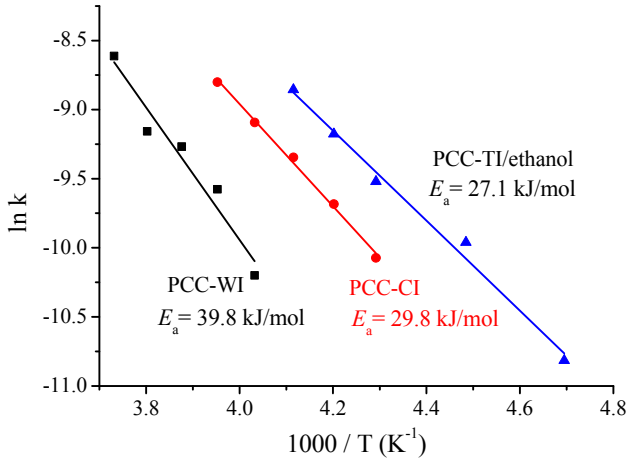

Fig. 5. Arrhenius plots of ln *r* versus 1/T over the Pd-Cu-Cl_x/Al_2O_3 catalysts for the CO oxidation under 1500 ppm CO and ~3.1% moisture/air.

To further know the effect of the preparation method of catalyst on its kinetic character of CO oxidation, the apparent activation energies (E_a) for CO oxidation were calculated based on the Arrhenius plots of ln*r* versus 1/T(K) (Fig. 5), in which the reactant gas of 0.15%CO-3.1%H_2O/Air was used. The reaction rates (*r*) were tested at differential mode with the CO conversion of < 15%. As shown in Fig. 5, E_a over the PCC-WI catalyst was 39.8 kJ/mol, much higher than that over the PCC-CI (29.8 kJ/mol) and PCC-TI/ethanol (27.1 kJ/mol) catalysts. Among the E_a values for the

three catalysts, that over PCC-TI/ethanol was the lowest. It clearly indicates that the PCC-TI/ethanol catalyst prepared by the two-step impregnation method is the most excellent catalyst for low temperature CO oxidation, compared with PCC-WI and PCC-CI. That is to say, the preparation method has a significant influence on the catalytic performance of the Pd-Cu-Cl_x/Al_2O_3 catalyst by varying the reactivity of active sites or its kinetic behaves.

3.5. Catalyst characterization

XRD and FT-IR tests of pre-synthetized $Cu_2Cl(OH)_3$ species. To evidence that the $Cu_2Cl(OH)_3$ phase was pre-synthetized successfully, the XRD and FT-IR spectra of pre-synthesized $Cu_2Cl(OH)_3$ were tested and shown in Fig. 6, which are similar to that reported.[24] In the FT-IR spectrum of $Cu_2Cl(OH)_3$ (Fig. 6A), the two absorption peaks at 3447 and 3358 cm^{-1} are ascribed to the hydroxyl stretching modes $\nu_1(O_1\text{-}H_1)$/$\nu_1(O_{2/3}\text{-}H_{2/3})$ of the $Cu_2Cl(OH)_3$, the peaks at 988−923 cm^{-1} are related to the δ_1(Cu-O-H) modes, and Cu-O related modes ν_s(O-Cu-O) and ν_1(O-Cu-O) were observed at 587 and 516 cm^{-1}, respectively. In the XRD pattern of $Cu_2Cl(OH)_3$, the five main diffraction peaks at 2θ = 16.19°, 30.95°, 39.75°, 50.46° and 53.75° are indexed to the peaks of chinoatacamite $Cu_2Cl(OH)_3$ (JCPDS 50-1559). Based on the results of FT-IR and XRD measurements, it can be confirmed that the $Cu_2Cl(OH)_3$ has been synthesized successfully.

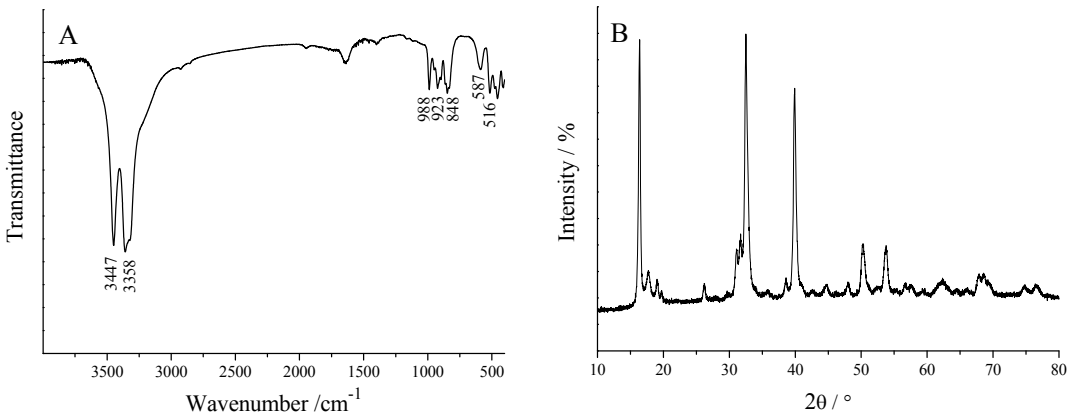

Fig. 6. (A) FTIR and (B) XRD spectra of pre-synthetized $Cu_2Cl(OH)_3$.

The $Cu_2Cl(OH)_3$/Al_2O_3 samples with different Cu loadings were prepared by the impregnation method and calcined at 300 °C, and their FT-IR spectra are shown in Fig. 7. Unlike the IR

spectrum of pure Al_2O_3 (Fig. 7a), the absorption peaks at 3447 and 3358 cm^{-1} in the IR spectra of $Cu_2Cl(OH)_3/Al_2O_3$ samples are ascribed to the hydroxyl stretching modes $\nu_1(O_1\text{-}H_1)/\nu_1(O_{2/3}\text{-}H_{2/3})$ of the $Cu_2Cl(OH)_3$. When Cu loading was 3.3wt.% (Fig. 7b), the intensities of the absorption peaks at 3447 and 3358 cm^{-1} were very weak, and when the Cu loading was increased from 3.3wt.% to 13.2wt.%, the intensities of these two absorption peaks were increased gradually. These results show that $Cu_2Cl(OH)_3$ on Al_2O_3 has survived after the impregnation and 300 °C calcination.

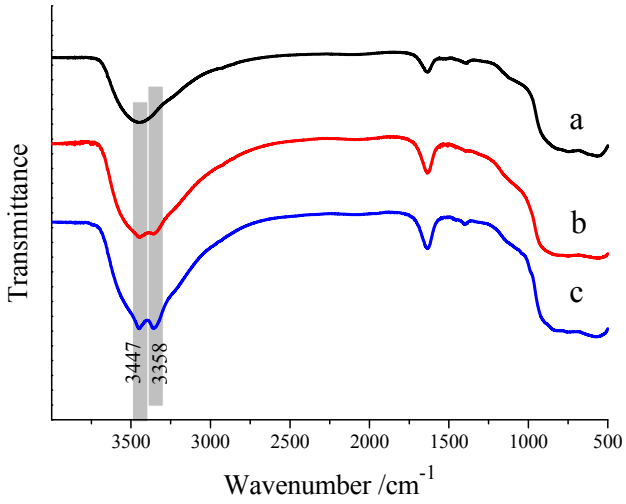

Fig. 7. FT-IR spectra of (a) Al_2O_3, (b) $Cu_2Cl(OH)_3/Al_2O_3$ (3.3wt%Cu) and (c) $Cu_2Cl(OH)_3/Al_2O_3$ (13.2wt%Cu).

ICP-OES and BET surface area. Table 1 presented the compositions of Pd and Cu in the catalysts, and the Pd content was ~1.6 wt.% and the Cu content was ~3.2 wt.% for the four samples, which were close to 1.7wt.% Pd and 3.3.wt.% Cu in the synthesis solution. These results showed that Cu and Pd were perfectly supported on the Al_2O_3 surface by the WI, CI and TI methods.

Table 1. Compositions, surface areas (S_{BET}) and $Cu_2Cl(OH)_3$ sizes of PCC catalysts

Catalyst	In solution (wt%)		In solid (wt%) [a]		S_{BET} (m^2/g)	$Cu_2Cl(OH)_3$ size (nm) [b]
	Cu	Pd	Cu	Pd		
PCC-WI	3.3	1.7	3.24	1.57	126	34
PCC-CI	3.3	1.7	3.21	1.51	129	16
PCC-TI/methanol	3.3	1.7	3.19	1.58	137	19
PCC-TI/ethanol	3.3	1.7	3.15	1.57	139	17

[a] Determined by ICP-OES method. [b] Calculated by Scherrer equation based on the diffraction peak of the (101) facet of $Cu_2Cl(OH)_3$.

Compared with the surface area (194 m^2/g) of Al_2O_3 bare support, the surface areas of PCC-WI, PCC-CI and PCC-TI were decreased after supporting Pd and Cu components, which may be resulted from the partial blocking of the pores of Al_2O_3 by the Pd and Cu species. The BET surface area of PCC-TI/methanol was 137 m^2/g, closing to that of PCC-TI/ethanol (139 m^2/g), which indicated the surface area of PCC-TI catalysts were insignificantly influenced by the organic solvent.

XRD analysis. As shown in Fig. 8, in the XRD patterns of four Pd-Cu-Cl_x/Al_2O_3 catalysts, only the diffraction peaks of alumina support and $Cu_2Cl(OH)_3$ could be observed. The diffraction peaks of Pd species were hardly discerned in the all samples, which indicated a high dispersion of Pd species on alumina or below the detection limit of XRD. The diffraction peaks of $Cu_2Cl(OH)_3$ species, the active copper phase in Pd-Cu-Cl_x/Al_2O_3, could be observed clearly in the all samples. The mean crystalline sizes of $Cu_2Cl(OH)_3$ are shown in Table 1. Comparing with the size (34 nm) of the $Cu_2Cl(OH)_3$ species in the PCC-WI catalyst, its sizes in PCC-CI and PCC-TI catalysts were smaller, such as, the one in PCC-CI catalyst was 16 nm, and these in PCC-TI/methanol and PCC-TI/ethanol catalysts were 19 nm and 17 nm, respectively. Those results above show that, different preparation methods can affect obviously the dispersion of $Cu_2Cl(OH)_3$ phase in the Pd-Cu-Cl_x/Al_2O_3 catalyst or its size, for instance, the X-ray diffraction peaks of $Cu_2Cl(OH)_3$ in the PCC-TI and PCC-CI samples were weaker and broader, indicating that its dispersion in PCC-CI and PCC-TI were higher than that in PCC-WI catalyst. The high catalytic activity of the PCC-TI samples should be attributed to the smaller sizes of its $Cu_2Cl(OH)_3$ active phase.[19]

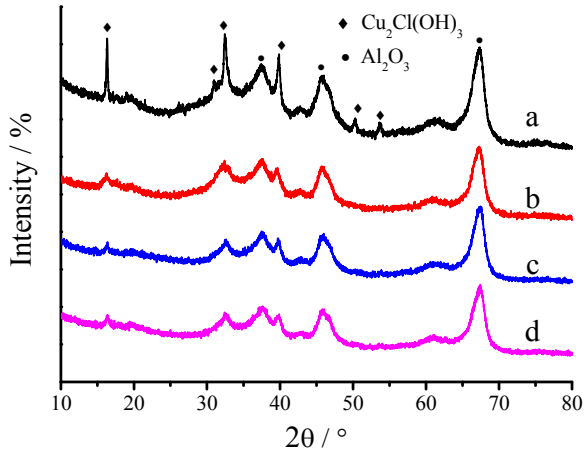

Fig. 8. XRD patterns of (a) PCC-WI, (b) PCC-CI, (c) PCC-TI/methanol, and (d) PCC-TI/ethanol.

H_2-TPR experiment. In the TPR profile of $PdCl_2/Al_2O_3$ catalyst (Fig. 9), a negative peak at 105 °C is attributed to a decomposition of palladium hydride.[29] The TPR profiles of $CuCl_2/Al_2O_3$ exhibits two reduction peaks at 280 °C and 360 °C. The former is related to the reduction of Cu^{2+} to Cu^{+}, and the latter results from the reduction of Cu^{2+} to Cu^{0}.[30]

There are two reduction peaks at 160 and 285 °C in the TPR profiles of the PCC-WI catalyst. The low temperature peak is related to the co-reduction of Pd and Cu species and the peak at 285 °C is ascribe to the reduction of isolated Cu species that has no interaction with the Pd species.[19] In the TPR profile of PCC-CI catalyst, only one reduction peak at 130 °C can be observed, and should be ascribed to the co-reduction of Pd and Cu species on the catalyst surface. And the reduction peak of bulk Cu species could be observed at >180 °C.

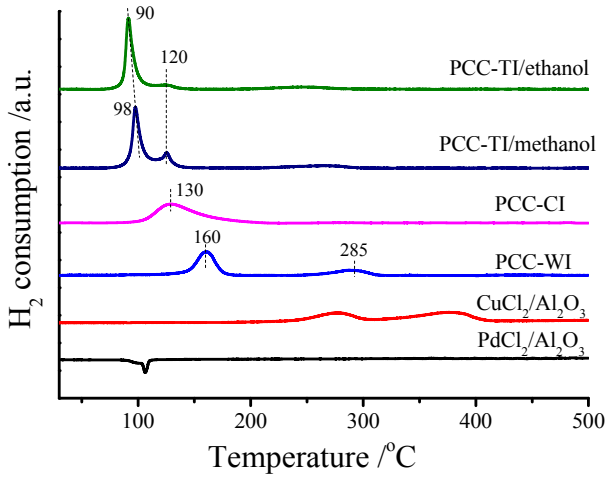

Fig. 9. TPR profiles of PCC-TI/ethanol, PCC-TI/methanol, PCC-CI, PCC-WI, $CuCl_2/Al_2O_3$ and $PdCl_2/Al_2O_3$ ($CuCl_2/Al_2O_3$ and $PdCl_2/Al_2O_3$ were prepared by WI method in the H_2O solvent).

The TPR profiles of PCC-TI catalysts are very different from those of PCC-WI and PCC-CI. In the TPR profiles of PCC-TI catalysts, two reduction peaks are located at 90-100 and 120 °C (Fig. 9). To clarify the attribution of these two reduction peaks of PCC-TI, the samples with different Cu and Pd loadings were prepared for the TPR experiments. The results in Fig. 10A show that, with the increase of Cu loading in the Cu-1.7wt.%Pd catalysts, the reduction peaks of PCC-TI/ethanol shifted to higher temperature and the reduction peak area was increased significantly. When the Cu loading was increased to 6.6wt.% in the Cu-1.7wt.%Pd sample, its γ peak appeared at 380 °C.

When the Cu loading was fixed to be 6.6wt.%, with an increase in Pd loadings in the PCC catalysts, the α peak shifted to lower temperature and its reduction peak area was increased gradually, but the γ peak was hardly changed (Fig. 10B). These results demonstrate that the sharp α peak should be related to the co-reduction of the Pd and Cu species on the catalyst surface, the β peak might be associated with the reduction of surface Cu species near Pd species, and the γ peak should be ascribed to the reduction of bulk Cu species. For the 6.6wt%Cu-0.8wt%Pd catalyst, its TPR curve is similar to that of $CuCl_2/Al_2O_3$ sample and different from these of the other 6.6wt%Cu-Pd catalysts, which shows that the presence of Pd promotes the reduction of Cu^{2+} ions and if the Pd loading is very low, this promotion of Pd would be unobvious. For the PCC-TI catalysts prepared by the two-step impregnation method with different alcohol solvents, their TPR curves are similar (Fig. 9), indicating that the reducibility of PCC-TI catalyst is hardly affected by the alcohol solvent.

The results mentioned above show that, the interaction between the copper and palladium species in the PCC-TI catalysts was stronger, and the presence of Pd can promote the reduction of Cu^{2+} ions, compared with PCC-WI and PCC-CI catalysts. For the PCC-TI/ethanol prepared in the ethanol solvent, it possesses lower reduction temperature (top temperature of α peak was 90 °C) and stronger interaction between Cu species and Pd species, that is, the α peak area of

PCC-TI/ethanol is larger than that of PCC-TI/methanol, resulting in its higher catalytic activity for the CO oxidation.

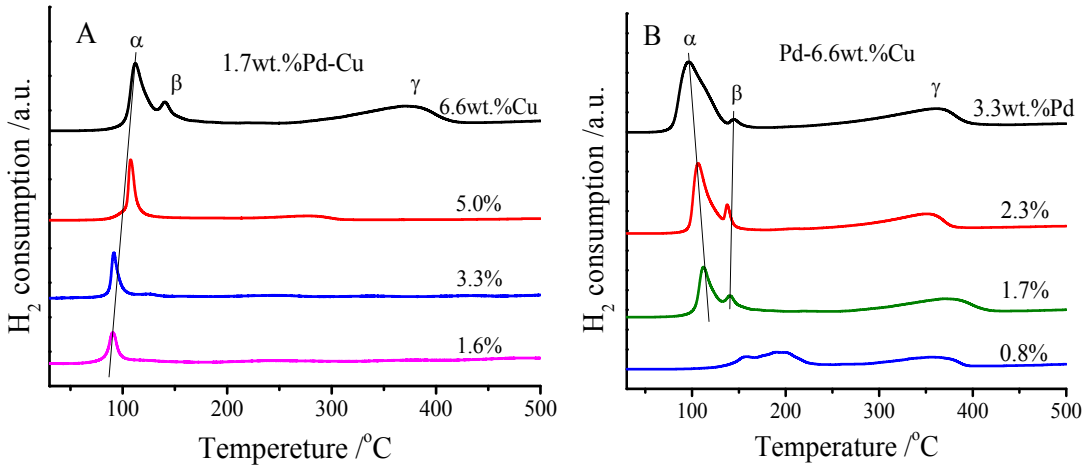

Fig. 10. TPR profiles of PCC-TI/ethanol of (A) (1.6-6.6)wt.%Cu-1.7wt.%Pd, and (B) 6.6wt.%Cu-(0.8-3.3)wt.%Pd.

3.6. *In situ* DRIFTS of the surface reaction and CO → CO_2 reaction on the Pd site

Fig. 11 shows the DRIFTS spectra of the catalysts in the mixed gases of 0.15%CO-20%O_2-3.1%H_2O/N_2. The absorption peaks at 2300-2400 cm^{-1} should be associated with the gaseous CO_2, the peaks at 1600-1700 cm^{-1} might be ascribed to −OH groups.[31,32] The peaks near 2110 cm^{-1} could be related with Cu^{+}-CO complex, the peaks at 1930-1940 cm^{-1} should be assigned to bridged carbonyl ligands in Pd^{+} complexes (Pd^{+}-CO), the weak peaks at 1990-2000 cm^{-1} are related with bridge-bonded CO on metallic palladium (Pd_2-CO), the peaks at 2162 cm^{-1} are associated with terminal CO groups in Pd^{2+} complexes (Pd^{2+}-CO).[33,34] The strong peaks at 1822 cm^{-1} are related to triply bonded CO on metallic Pd (Pd_3-CO). The peaks at 1200-1600 cm^{-1} are associated with carbonate species.[35]

As shown in the IR spectra of the PCC-TI/ethanol catalyst (Fig. 11A), the intensities of Pd_2-CO peak and Pd^{+}-CO peak were decreased significantly, and the absorption peaks of Pd_3-CO, OH group and gaseous CO_2 were increased gradually, with an increase in the reaction time.

The DRIFTS spectra of the PCC-CI catalyst are shown in Fig. 11B, the absorption peaks of CO adsorbed (except Pd_3-CO) were decreased significantly and the peaks of adsorbed −OH groups

were increased gradually, with the reaction time. Comparing with the IR spectra of the PCC-TI/ethanol catalyst, some differences can be found: trace of Cu^{+}-CO peak was observed at the beginning of reaction, but this peak could not be seen in the IR spectra of PCC-TI/ethanol, which demonstrates that the oxidation rate of Cu^{+} species on the PCC-CI surface was slower than that on PCC-TI/ethanol; the absorption bands of carbonates could be observed clearly and increased with the reaction time, which suggests the carbonate species was easily accumulated on the PCC-CI surface, resulting in the reduction of its catalytic activity and stability; the absorption peak of gaseous CO_2 at 2300-2400 cm^{-1} declined gradually and disappeared with the reaction time, which shows that this catalyst has been deactivated to fail to produce CO_2 by CO oxidation.

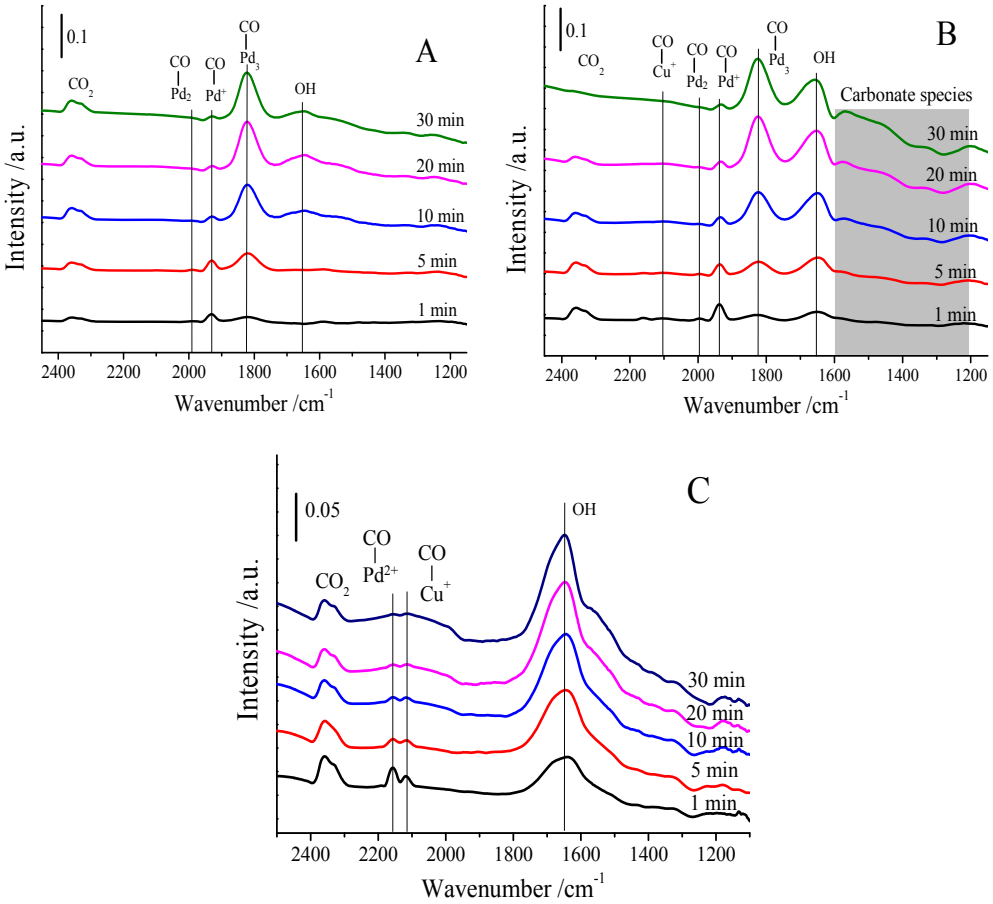

Fig. 11. *In situ* DRIFTS spectra of CO adsorbed over (A) PCC-TI/ethanol, (B) PCC-CI and (C) PCC-WI in the mixed gas of 0.15%CO-20%O_2-3.1%H_2O/N_2 at 25 °C.

Being quite different from the IR spectra of PCC-TI/ethanol and PCC-CI catalysts, in the IR absorption spectra of the PCC-WI catalyst (Fig. 11C), the IR absorption peaks of Cu^{+}-CO and Pd^{2+}-CO existed, and the peaks of Pd^{+}-CO could not be observed. It was reported that the Pd^{+} sites

have higher activity than the Pd^{2+} sites for the CO oxidation, CO adsorbed on Pd^{+} sites could be oxidized to CO_2 more easily than CO adsorbed on Pd^{2+} sites.[22] This is the reason that the PCC-TI/ethanol and PCC-CI catalysts exhibited higher catalytic activity than the PCC-WI catalyst for the CO oxidation.

Although there are differences in DRIFTS spectra described above for CO oxidation over the Pd-Cu-Cl_x/Al_2O_3 catalysts prepared by the different methods, we would like to look at the similarity of them to understand the general catalytic mechanism. As shown in Figure 10, −OH groups, metallic Pd^0(Pd_3-CO) and Pd^{+} complexes (Pd^{+}-CO) are common species in the catalytic oxidation process of CO. In our previous theoretical work, we have studied the catalytic oxidation mechanism of CO on the Pd-Cu-Cl_x/Al_2O_3 catalyst. We found that the Pd catalysis is the main active sites of CO and the Cu catalysis is the main active sites of O_2.[23] For the Cu catalysis, O_2 was absorbed on Cu^{+} to form Cu^{2+}-O_2, and then O atom was transferred to Pd^0-CO by the help of redox process, resulting in the CO oxidation and the formation of Pd^{+} species. More information could be obtained in Ref. 23. For the Pd catalysis as the active sites of CO, we took DFT calculation to further study the catalytic cycle of CO oxidation on the Pd species, to reveal the possibly evolutive routes of the common species observed in the DRIFTS spectra. The main energy change and corresponding structures are shown in Fig. 12.

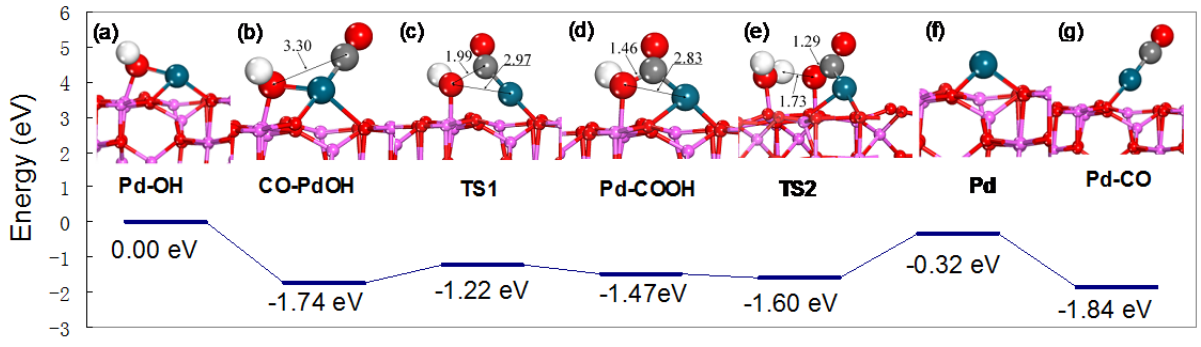

Fig. 12. The main energy change and corresponding structures for the catalytic cycle of CO → CO_2 reaction on the Pd species. (a) Structure of Pd-OH, (b) structure of CO-PdOH, (c) transition state of the CO-PdOH → *cis*-PdCOOH reaction, (d) structure of *cis*-PdCOOH, (e) transition state of the *cis*-PdCOOH + −OH → Pd-CO_2 + −H_2O reaction, (f) adsorption state of Pd^0, and (g) structure of Pd-CO. (Bond length is in Å. O atoms are red, Al atoms are pink, H atoms are white, Al atoms are pink, Pd atoms are dark blue).

In the presence of –OH dissociated from H_2O, $PdCl_2$ is converted to Pd-OH (Fig. 12a). CO adsorbs on PdOH to form the CO-Pd-OH species (Fig. 12b), which is corresponding to the Pd^+-CO peak in DRIFTS spectra, while this structure turns to *cis*-PdCOOH intermediate with an energy barrier of 0.52 eV (Fig. 12b). Next, the *cis*-PdCO-OH (Fig. 12d) directly dissociates −H to the nearest surface −OH to form adsorbed H_2O and Pd-CO_2, and then releases CO_2 to the gas phase (Fig. 12e), while Pd^0 is produced (Fig. 12f). After CO adsorption, Pd^0 turns to Pd-CO (Fig. 12g) with adsorption energy of 1.52 eV. The evidence of Pd^0 is shown as the CO-Pd_3 absorption peak at 1822 cm^{-1} in DRIFTS spectra. These results show that theoretical results are well correlated to the DRIFTS spectra, and are mutually validated with each other.

H_2O plays a subtle role in the CO catalytic oxidation over the Pd-Cu-Cl_x/Al_2O_3 catalyst. The DFT study showed that the trace of H_2O on dry γ-Al_2O_3 surface could work as a part of the catalytic cycle for low temperature CO oxidation, but when the moisture was excessive, the dissociated −H and −OH would occupy the active sites of Pd and Cu on the Al_2O_3 surface as poisonous species, resulting in a deactivation of the catalyst for the CO oxidation. The results of DRIFTS study for the surface reaction show that, the intensities of −OH groups on three catalysts prepared by the different methods. The intensity of −OH groups on the surface of PCC-TI/ethanol was weaker than that of PCC-WI and PCC-CI, which clearly confirms that moderate −OH groups are advantageous to CO oxidation, according with the results of DFT study.

The DRIFTS results above also show that, carbonate species was hardly accumulated on the PCC-TI/ethanol catalyst, in which the oxidation rate of Cu^+ to Cu^{2+} was faster than that in PCC-CI catalyst, indicating that the PCC-TI/ethanol catalyst has better activity and stability than the other catalysts.

4. Conclusions

In summary, the Pd-Cu-Cl_x/Al_2O_3 catalysts were prepared by three different preparation methods for low temperature CO oxidation. And PCC-TI catalysts prepared by the two-step

impregnation (TI) method showed the outstanding catalytic activities and stabilities compared with the PCC-WI and PCC-CI catalysts prepared by the wet impregnation (WI) and NH_3 coordination-impregnation (CI) methods, respectively. Among the four catalysts, the reaction temperature of 100% CO conversion was the lowest (only at 10 °C) in the presence of ~3.1% moisture over the PCC-TI/ethanol catalyst and its E_a was also the lowest (27.1 kJ/mol). The PCC-TI catalysts exhibits the excellent catalytic activity, which should be ascribed to the higher dispersion of $Cu_2Cl(OH)_3$ phase on its surface and the stronger interaction between copper and palladium species. For the PCC-TI catalysts, the solvent in the synthesis solution would affect its catalytic performance. The PCC-TI/ethanol prepared in the ethanol solvent showed a higher activity than PCC-TI/methanol, which resulted from the much stronger interaction between the copper and palladium species.

The −OH groups on Pd-Cu-Cl_x/Al_2O_3 catalyst surface played important roles in the catalytic oxidation of CO, moderate −OH groups can work as parts of the catalytic cycle as an important species for low temperature CO oxidation, and excessive −OH groups could occupy the active sites on the Al_2O_3 surface, resulting in a deactivation of catalyst. Compared with PCC-CI catalyst, carbonate species is hardly accumulated on the PCC-TI/ethanol surface, which results in its higher stability. High CO concentration played a negative influence on the CO conversion, might be originated from the competitive adsorption and the covering of carbonates on the catalyst surface. We took DFT calculation to study the catalytic cycle of CO oxidation on the Pd species, to reveal the possibly evolutive routes for the common species observed in the DRIFTS spectra.

Acknowledgements

This project was financially supported by the National Natural Science Foundation of China (21273150, 21203119), the National Basic Research Program of China (2013CB933201), the national high technology research and development program of China (2011AA03A406, 2012AA062703), the Shanghai Natural Science Foundation (12ZR1430800), and the Shanghai

Innovation Program (12YZ161).

Notes and References

1. M. Chen, D. Goodman, *Science*, 2004, **306**, 252.
2. C. Jones, S. H. Taylor, A. Burrows, M. J. Crudace, C. J. Kiely, G. J. Hutchings, *Chem. Commun.,* 2008, 1707.
3. J. Y. Luo, M. Meng, X. Li, X. G. Li, Y. Q. Zha, T. D. Hu, Y. N. Xie, J. Zhang, *J. Catal.,* 2008, **254**, 310.
4. X. Xie, Y. Li, Z. Q. Liu, M. Haruta, W. Shen, *Nature*, 2009, **458**, 746.
5. Y. Yu, T. Takei, H. Ohashi, H. He, X. Zhang, M. Haruta, *J. Catal.,* 2009, **267**, 121.
6. D. R. Merrill, C. C. Scalione, *J. Am. Chem. Soc.,* 1921, **43**, 1982.
7. F. Grillo, M. M. Natile, A. Glisenti, A, *Appl. Catal., B,* 2004, **48**, 267.
8. E. C. Njagi, C. H. Chen, H. Genuino, H. Galindo, H. Huang, S. L. Suib, *Appl. Catal., B,* 2010, **99**, 103.
9. M. Haruta, N. Yamada, T. Kobayashi, S. Iijima, *J. Catal.,* 1989, **115**, 301.
10. G. Y. Wang, H. L. Lian, W. X. Zhang, D. Z. Jiang, T. H. Wu, *Kinet. Catal.,* 2002, **43**, 433.
11. J. M. Soares, M. Hall, M. Cristofolini, M. Bowker, *Catal. Lett.,* 2006, **109**, 103.
12. I. D. Gómez, I. Kocemba, J. M. Rynkowski, *Appl. Catal., B,* 2009, **88**, 83.
13. S. H. Choi, J. S. Lee, *React. Kinet. Catal. Lett*., 1996, **57**, 227.
14. J. S. Lee, S. H. Choi, K. D. Kim, M. Nomura, *Appl. Catal., B,* 1996, **7**, 199.
15. E. D. Park, J. S. Lee, *J. Catal.,* 1998, **180**, 123.
16. E. D. Park, S. H. Choi, J. S. Lee, *J. Phys. Chem. B,* 2000, **104**, 5586.
17. E. D. Park, J. S. Lee, *J. Catal.,* 2000, **193**, 5.
18. A. J. Dyakonov, *J. Appl. Catal., B,* 2003, **45**, 257.
19. Y. Shen, G. Lu, Y. Guo, Y. Wang, *Chem*. *Commun.,* 2010, **46**, 8433.
20. L. Wang, Y. Zhou, Q. Liu, Y. Guo, G. Lu, *Catal. Today,* 2010, **153**, 184.
21. Y. Shen, Y. Guo, L. Wang, Y. Wang, Y. Guo, X. Gong, G. Lu, *Catal. Sci. Technol.,* 2011, **1**, 1202.
22. Y. Shen, G. Lu, Y. Guo, Y. Wang, Y. Guo, X. Gong, *Catal. Today,* 2011, **175**, 558.
23. C. Shen, H. Li, J. Yu, G. Wu, D. Mao, G. Lu, *ChemCatChem.,*2013, **5**, 2813.

24. W. Wei, P. Gao, J. Xie, S. Zong, H. Cui, X. Yue, *J. Solid State Chem.,* 2013, **204**, 305.
25. G. Kresse, D. Joubert, *Phys. Rev., B,* 1999, **59**, 1758.
26. M. Digne, P. Sautet, P. Raybaud, P. Euzen, H. Toulhoat, *J. Catal.,* 2004, **226**, 54.
27. K. D. Kim, I. S. Nam, J. S. Chung, J. S. Lee, S. G. Ryu, Y. S. Yang, *Appl. Catal., B,* 1994, **5**, 103.
28. D. J. Koh, J. H. Song, S. W. Ham, I. S. Nam, R. W. Chang, E. D. Park, J. S. Lee, Y. G. Kim, *Korean J. Chem. Eng.* , 1997, **14**, 486.
29. W. J. Shen, M. Okumura, Y. Matsumura, M. Haruta, M. *Appl. Catal. ,A,* 2001, **213**, 225.
30. A. Rouco, *J. Catal.,* 1995, *157*, 380.
31. H. Zhu, Z. Qin, W. Shan, W. Shen, J. Wang, *J. Catal.,* 2004, **225**, 267.
32. H. Zhu, Z. Qin, W. Shan, W. Shen, J. Wang, *J. Catal.,* 2005, **233**, 41.
33. K. I. Choi, M. A.Vannice, *J. Catal.,* 1991, **127**, 489.
34. K. I. Choi, M. A. Vannice, *J. Catal.,* 1991, **131**, 22.
35. O. Pozdnyakova, D. Teschner, A. Wootsch, J. Kröhnert, B. Steinhauer, H. Sauer, L. Toth, F. Jentoft, A. Knop-Gericke, Z. Paál, *J. Catal.,* 2006, **237**, 1.